3. T. G. Gibson, *Geol. Soc. Amer. Bull.* **81**, 1813 (1970).
4. G. Brown, J. A. Catt, A. H. Weir, *Mineral. Mag.* **37**, 480 (1969).
5. M. N. Bramlette and E. Posnjak, *Amer. Mineral.* **18**, 167 (1933); K. S. Deffeyes, *J. Sediment. Petrol.* **29**, 602 (1959); J. C. Hathaway and P. L. Sachs, *Amer. Mineral.* **50**, 852 (1965); R. L. Hay, *Geol. Soc. Amer. Spec. Pap. 85* (1966).
6. R. L. C. Enright, Jr., personal communication (1968); thesis, Rutgers University (1969).
7. S. D. Heron, Jr., *Geol. Soc. Amer. Annu. Meeting Program* (1962), p. 71A; S. D. Heron, Jr., G. C. Robinson, H. S. Johnson, Jr., *S.C. State Develop. Board Div. Geol. Bull. 31* (1965).
8. We thank S. D. Heron, Jr., for restudying these sediments at our request and providing new x-ray data on their mineralogy.
9. C. E. Weaver, *Southeast. Geol.* **9**, 57 (1968).
10. W. R. Reynolds, *J. Sediment. Petrol.* **40**, 829 (1970)
11. R. E. Grim, *Miss. State Geol. Surv. Bull. 30* (1936).
12. E. G. Wermund and R. J. Moiola, *J. Sediment. Petrol.* **36**, 248 (1966).
13. P. Brönnimann and D. Rigassi, *Eclogae Geol. Helv.* **56**, 193 (1963).
14. We thank Dr. E. Gasche for providing these samples for study.
15. T. G. Gibson, J. E. Hazel, J. F. Mello, *U.S. Geol. Surv. Prof. Pap. 600-D* (1968), p. 222.
16. M. N. Bramlette, personal communication (1969).
17. JOIDES, *Science* **150**, 709 (1965).
18. M. N. Bramlette and F. R. Sullivan, *Micropaleontology* **7**, 129 (1961).
19. W. K. Pooser, *Univ. Kans. Paleontol. Contrib. Arthropoda*, Art. 8 (1965).
20. N. L. Taliaferro, *Calif. Univ. Dep. Geol. Sci. Bull.* **23**, 1 (1933); M. N. Bramlette, *U.S. Geol. Surv. Prof. Pap. 212* (1946).
21. W. R. Riedel, *Soc. Econ. Paleontol. Mineral. Spec. Publ.* **7**, 80 (1959).
22. T. C. Moore, Jr., *Geol. Soc. Amer. Bull.* **80**, 2103 (1969).
23. R. A. Daly, *Igneous Rocks and the Depths of the Earth* (McGraw-Hill, New York, 1933).
24. R. S. Dietz and J. C. Holden, *J. Geophys. Res.* **75**, 4939 (1970); W. A. Berggren and J. D. Phillips, *Symp. Geol. Libya*, in press.
25. H. J. MacGillavry, *Proc. Koninklijke Ned. Akad. Wetensch. Ser. B* **73**, 64 (1970).
26. J. Ewing, C. Windisch, M. Ewing, *J. Geophys. Res.* **75**, 5645 (1970).
27. We thank R. Cifelli, J. E. Hazel, and W. G. Melson for reviewing the manuscript. M. N. Bramlette provided valuable assistance in nannoplankton identification and biostratigraphy.

23 November 1970

Cosmic-Ray Tracks in Plastics: The Apollo Helmet Dosimetry Experiment

Abstract. *Counts of tracks from heavy cosmic-ray nuclei in helmets from Apollo missions 8 and 12 show variations caused by solar modulation of the galactic cosmic-ray flux. Specific estimates of the biological damage to certain nonreplaceable cells by track-forming particles during these space missions indicate that the fraction of deactivated cells could range from a lower limit of* 3×10^{-7} *to an upper limit of* 1.4×10^{-4}.

In passing through condensed matter, a heavily ionizing particle can produce unique effects by creating a narrow, roughly cylindrical region that is crowded with ionization and excitation, with atomic displacements and broken bonds (*1*). Unfortunately our minute knowledge of the biological effects of heavy ion irradiations stands in striking contrast to the extensive documentation that exists of the effects produced by more usual, randomly dispersed defects such as are caused by β or γ radiation. Although it has been demonstrated that heavy ions can have lethal effects upon colony-forming cells (*2*, *3*), for nonregenerative human cells such information is totally lacking, difficult to obtain, and hence unlikely to be available soon. Because of this gap in our knowledge and because of the probable loss by space travelers of irreplaceable cells by heavy ions in the cosmic rays, such particles have been monitored on the Apollo 8 and 12 missions by using Apollo helmets as heavy particle dosimeters.

The Apollo helmets consist of Lexan polycarbonate, a material that records the tracks of particles whose ionization level lies above that produced by neon at ~ 7 Mev per nucleon (*4*), essentially the same level as corresponds to inactivation with unit efficiency of human kidney T1 cells by a particle that traverses the cell nucleus (*2*). Because of the approximate identity of these two thresholds—for track formation and for cell destruction (at least for T1 cells)—Lexan is an appropriate detector material for assessing the dose of biologically destructive particles to which the astronauts were exposed.

The helmets used for this experiment include the one worn by astronaut Lovell on Apollo 8, all three of the Apollo 12 helmets, and a control helmet that was exposed to cosmic rays at a balloon altitude of 138,000 feet (41,000 m) at Fort Churchill. The helmets were stored in the dark to avoid ultraviolet enhancement effects (*5*). Later they were chemically etched to reveal tracks (*6*) with a stirred 1 : 1 solution (by volume) of ethanol and 6.25*N* NaOH at 23°C for 196 hours, a period sufficient to remove a veneer of ~ 80 μm of plastic (~ 4 percent of the initial thickness) and to develop tracks similar to those shown in Fig. 1. The helmets themselves were used as etching tanks; only ~ 600 cm^2 of the forward-facing portions of the helmets were etched to avoid damage to the headrest and other fittings. The etched portions were replicated with silicone rubber (*7*), and the gold-coated replicas [see figures 1 and 3 in (*7*)] were scanned in a stereomicroscope at a magnification of × 14. Features with vertical relief down to ~ 15 μm were readily visible under our viewing conditions, a height that for a track at 45° corresponds to a total etched length of ~ 135 μm. Although our cutoff for track observation is not perfectly sharp, we can use our estimate for effective value of 135 μm of minimum total etched length to show (*8*) that the tracks we observe correspond entirely to nuclei of atomic number (Z) ≥ 10 and that from the known abundances in this charge region (*9*) most of these will be iron or iron group ($24 \leq Z \leq 28$) nuclei.

The results summarized in Table 1 show that the Apollo 12 helmets experienced nearly three times the integrated flux of heavily ionizing cosmic rays as did the Apollo 8 helmet. Even when allowance is made for the different lengths of the two missions, the track formation rate on Apollo 12 is still significantly higher (by a factor of 2.0). The track formation rate in the balloon-flown helmet was 3.1 times higher than that on the Apollo 8 mission. On the Apollo 12 mission, helmets 504 and 506 were in the lunar module for 25 hours and were outside the lunar module, during the astronauts' extravehicular activity, for nearly 8 hours. During this 33-hour period the average thickness of shielding material surrounding the helmet is considerably reduced relative to the environment in the command module, where the remainder of the trip was spent. This different environment produced no statistically meaningful difference between the track densities in Gordon's helmet [1.41 (± 0.15)] and those in Bean's and Conrad's [1.51 (± 0.11)], although the possibility of as much as a 30 percent increase is allowed by standard deviation limits. Two relevant considerations are that the lunar module and extravehicular activity portions of the trip make up only 14 percent of the total time of 244.5 hours in space and that during the stay on or near the moon half of the incident cosmic rays

Table 1. Heavy cosmic-ray track densities and fluxes in Apollo helmets. Fluxes are calculated on the assumption of a solid angle of 2π at and near the moon or earth and of 4π in space between the moon and earth; this flux is the flux of particles capable of producing tracks that are >150 μm in length under the etching conditions that were used. CNM, Climax neutron monitor; CM, command module; LM, lunar module; LS, lunar surface; S.D., standard deviation.

Helmet	Location (CNM rate)	Track density per cm² (± S.D.)	Fluxes (track/cm²-sec-sr)		Relative to Apollo 12	
			Observed (± 10%)	Calculated (± 30%)	Observed (± 15%)	Calculated (± 15%)
		Apollo 8 (21–27 December 1968)				
057 (Lovell)	CM (3709)	0.56 (± .053)	0.765×10^{-7}	1.39×10^{-7}	0.49	0.66
		Apollo 12 (14–24 November 1969)				
007 (Gordon)	CM (3843)	1.41 (± .146)	1.56×10^{-7}	2.11×10^{-7}	1.00	1.00
504 (Bean)	CM, LM, LS	1.55 (± .154)	1.71×10^{-7}	$\approx 2.24 \times 10^{-7}$	1.09	≈ 1.06
506 (Conrad)	CM, LM, LS	1.47 (± .152)	1.62×10^{-7}		1.04	
		Fort Churchill balloon flight (11–12 July 1970)				
Control	2.5 g/cm² atmospheric depth (3715)	0.076 (± .012)	2.35×10^{-7}	2.36×10^{-7}	1.51	1.12

are shielded out by the moon itself.

We now assess whether the track accumulation rate from Apollo 8 (December 1968) to Apollo 12 (November 1969) can be explained by the effects of decreasing solar activity during this period of the present solar cycle—the so-called *solar modulation* of the galactic cosmic rays. During times of decreasing solar activity, the radially expanding irregularities in the solar magnetic field become progressively less effective in scattering back out of the solar system the low-energy cosmic-ray particles that are continually diffusing inward. The solar activity level was essentially the same for Apollo 8 and the balloon flight (July 1970). The difference in these fluxes is due to the overlying material: command module wall and atmosphere, respectively.

We have calculated both the absolute number of tracks that we should have expected and the variations over time as affected by solar modulation. We used known energy (*10*) and abundance (*9, 11*) spectra for heavy cosmic rays together with a modulation model (*12*) that correlates the variations in neutron monitor rates at Climax, Colorado, with the energy spectra for particles of given velocity and magnetic rigidity, and we allowed for slowing down (*13*) and loss by fragmentation (*14*) in inelastic collisions (*15*) while passing through the spacecraft walls. The thickness distribution of stopping material in the command module (*16*) was approximated as consisting of pure aluminum for purposes of calculating energy loss and deciding appropriate cross sections for inelastic collisions. Etching efficiencies were derived from unpublished calibration curves.

The results of these calculations are included in Table 1, along with the observations. Track density ratios from one mission to another should be more reliably calculable (expected to be good to ± 15 percent) as compared with the absolute fluxes (good to roughly ± 30 percent). Examination of Table 1 shows the agreement to be compatible with the estimated errors. The absolute number observed here of 0.56 (± 10 percent) per square centimeter for Apollo 8 should be compared with the observations of Benton *et al.* (*17*) on Lexan sheets that were attached to the space suit of astronaut Borman in the same flight. By using a different etch, ultraviolet sensitization, and scanning at a magnification of × 100, the found 0.62 (± 0.11) track/cm² on the basis of 34 tracks. When allowance is made for the differences in scanning and etching, this value would be reduced by approximately 10 percent, which is in complete agreement with 0.56 (± 0.06), if we neglect the effect of the possible difference in shielding of the two locations.

Since this experiment was primarily for personnel dosimetry purposes, the following comments are appropriate. When worn, the helmets give to a very high approximation the heavy particle dose incident on the head and face of the wearer. Of the 244.5 hours of the Apollo 12 mission, helmets 504 and 506 were worn approximately 8 hours, and the other helmets were worn for shorter periods. It follows that a 1 to 1 correspondence of track in helmet to biologically damaging particle in astronaut does not exist. We have found, however, as noted earlier, that the doses at the helmets were not very sensitive to position within the spacecraft or, in fact, to which spacecraft they were in but depend primarily

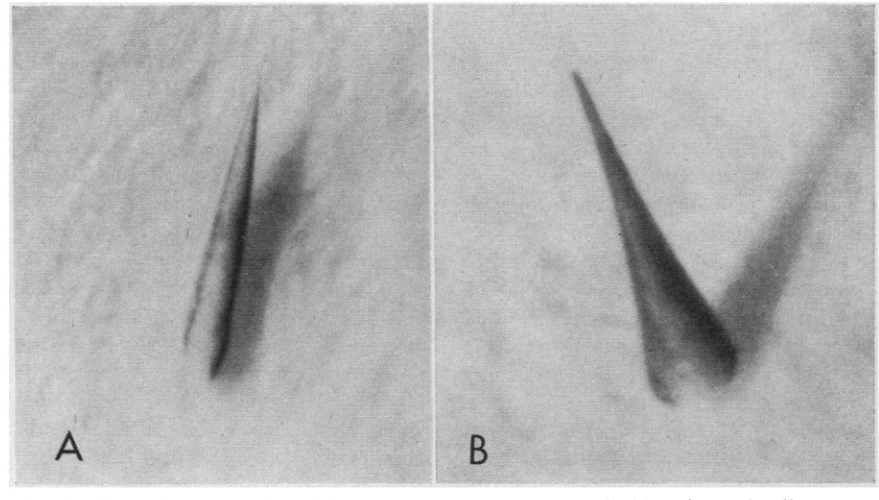

Fig. 1. Examples of tracks of heavy cosmic rays on the inside of an Apollo space helmet. (A) A track from a particle entering the helmet. (B) An ending track, from a particle that has crossed from the opposite side of the helmet and come to rest. The tracks are 500 and 700 μm in length, respectively.

Table 2. Estimates of cell loss fractions for Apollo 12 flight and hypothetical 2-year flight.

Cells	Cell diameter (μm)	Nuclear diameter (μm)	Fraction lost (parts per million)	
			Apollo 12 flight	2-Year flight*
Granular layer cerebellum	4	3.6	0.50–0.65	40–50
Light receptors	6×20	4	0.64–5.7	50–500
Cerebrum	19	4	2–14	16–120
Giant Betz	45	18	13–83	1,050–6,600
Anterior horn	70	25	26–200	2,000–16,000

* The flux was assumed to be the same as during the Apollo 12 flight.

on the solar activity at the time of the mission. For this reason, the dose of heavy particles experienced by the astronauts will in a statistical sense be well measured by the track density in the helmets.

Recalling our earlier observation that the track ionization threshold for Lexan is essentially the same as that for inactivating a T1 cell, we can attempt to calculate limits on the number of cells deactivated from the track density ρ and from assumptions based on limited and inexact biological evidence. A lower limit on the number of cells killed comes from Todd's observations (*2*) for human kidney cells that a heavy particle will cause a cell to cease to reproduce if it passes through a cell nucleus. With increasing ionization, the size of the region of damage is widened [as noted in (*2*) for ^{40}Ar irradiation], and a reasonable upper limit on the number of affected cells comes from the model that each cell that is penetrated will be killed, giving rise to a continuous column of dead cells for each such heavy particle. This behavior is made plausible by recent work by Haymaker *et al.* (*18*), who found track-like lesions consisting of columns of dead cells in brains of monkeys that had been exposed to primary cosmic rays. Although these lesions could, at least in part, have been of cosmic-ray origin, definite conclusions must await detailed experiments where tracks in suitable detectors can be lined up with the biological damage.

Limits on the fraction of cells killed can be determined if we know the cell size (in terms of the diameter D) and the track density ρ of heavily ionizing particles from Table 1. For the upper limiting case, the fraction of killed cells is $\pi\rho D^2/2$, the product of the projected cross-sectional area $\pi D^2/4$, and the line length per unit volume 2ρ. In converting from length in Lexan polycarbonate (specific gravity, 1.20) to biological matter, we multiply the line length by 1.2. An additional factor of 10/7 is included to allow for the fact that only 70 percent of the tracks crossing the etched surface are revealed. If d is the diameter of the nucleus, then $\pi\rho d^2/2$ gives a lower limit, on the criterion that a particle must pass through the cell nucleus. Since the spectrum of cell sizes, nuclear sizes, and volume fractions of cellular material are immense, we restrict our estimates to nonregenerative cells such as those in the retina and in the central nervous system. We take estimates of cell dimensions from several sources (*2*, *18*, *19*). For the cerebral cortex, we assume 10^{10} cells in a total volume of 300 cm^3 composed of 25 percent neurons and 75 percent glial and endothelial cells. The average diameter is then 19 μm, and we assume a nuclear diameter of 7 μm. In Table 2 the limits on cell loss from heavy cosmic-ray particles passing through any part of the cell (upper limit) or through the cell nucleus (lower limit) are given for the Apollo 12 flight and extrapolated to a flight of 2 years duration under the same conditions. Depending on cell size, the limits for fractional loss range from $\sim 4 \times 10^{-7}$ to 10^{-4} for Apollo 12.

Although these numbers are moderately small, assessing whether such damage is of importance is by no means simple, particularly since the damage is strongly concentrated at contiguous or nearby cells. On an extended space mission of, for example, 2 years duration (such as is being considered for Mars), Table 2 shows that the fraction killed could rise to 0.12 percent in the cerebral cortex, 0.05 percent in the retina, and more than 1.5 percent for some of the giant cells—numbers that may be highly worrisome since additional safe shielding would impose important weight considerations on spacecraft design.

The results here lead to the interesting apparent paradox that for extended space missions times of near maximum solar activity provide the greatest safety from heavy particles. This is because the increased flux of solar particles (in all but the most intense flares) is stopped by the rather modest shielding of the spacecraft, whereas the more penetrating galactic particles are decreased in number by the effects of solar magnetic field irregularities. Thus, from the standpoint of astronaut safety, the early 1980's would be superior to the latter half of the decade for a Mars voyage.

G. M. Comstock
R. L. Fleischer
W. R. Giard, H. R. Hart, Jr.
G. E. Nichols, P. B. Price*
General Electric Research and Development Center, Schenectady, New York 12301

References and Notes

1. R. L. Fleischer, P. B. Price, R. M. Walker, *Annu. Rev. Nucl. Sci.* **15**, 1 (1965); *Science* **149**, 383 (1965); *J. Appl. Phys.* **36**, 3645 (1965).
2. P. Todd, *Radiat. Res.* **7** (Suppl.), **196** (1967).
3. L. D. Skarsgard, B. A. Kihlman, L. Parker, C. M. Pujara, S. Richardson, *ibid.*, p. 208.
4. R. L. Fleischer, P. B. Price, R. M. Walker, E. L. Hubbard, *Phys. Rev.* **156**, 353 (1967).
5. W. T. Crawford, W. DeSorbo, J. S. Humphrey, *Nature* **220**, 1313 (1968).
6. R. L. Fleischer and P. B. Price, *Science* **140**, 1221 (1963).
7. ———, H. R. Hart, Jr., W. R. Giard, *ibid.* **170**, 1189 (1970).
8. As is clear from (*4*), for each heavy particle there is a maximum length over which the damage rate is above threshold, so that a track is formed and can be etched. The frequency of such tracks is proportional to this length (minus the 135 μm) and to the abundance of the particular heavy particle. Consequently, many of the iron tracks are revealed (lengths up to 8 mm) and few neon tracks (lengths $\sim$200 μm), even though their abundances in the cosmic radiation are approximately equal.
9. P. B. Price, R. L. Fleischer, D. D. Peterson, C. O'Ceallaigh, D. O'Sullivan, A. Thompson, *Phys. Rev. Lett.* **21**, 630 (1968); paper presented at the 11th International Conference on Cosmic Rays, Budapest, August 1969 [*Hung. Acta Phys.* **29** (Suppl. 1), 417 (1970)].
10. P. S. Freier and C. J. Waddington, *Phys. Rev.* **175**, 1641 (1968); G. M. Comstock, C. Y. Fan, J. A. Simpson, *Astrophys. J.* **155**, 609 (1969); T. T. von Rosenvinge, W. R. Webber, J. F. Ormes, *Astrophys. Space Sci.* **5**, 342 (1969) [note that in this paper the VH point (for very heavy cosmic-ray nuclei) of Comstock *et al.* is incorrectly plotted too low by a factor of 1.7].
11. M. G. Munoz and J. A. Simpson, paper presented at the 11th International Conference on Cosmic Rays, Budapest, August 1969 [*Hung. Acta Phys.* **29** (Suppl. 1), 325 (1970)].
12. K. C. Hsieh, *Astrophys. J.* **159**, 61 (1970); J. R. Wang, *ibid.* **160**, 261 (1970).
13. W. H. Barkas and M. J. Berger, *Nat. Aeronaut. Space Admin. Rep. SP-3013* (Office of Technical Services, Department of Commerce, Washington, D.C., 1964).
14. C. J. Waddington, *Astrophys. Space Sci.* **5**, 3 (1969).
15. F. F. Chen, C. P. Leavitt, A. M. Shapiro, *Phys. Rev.* **99**, 857 (1955); R. Goloskie and K. Strauch, *Nucl. Phys.* **29**, 474 (1962); P. Kirkby and W. T. Link, *Can. J. Phys.* **44**, 1847 (1966).
16. W. N. Hess, personal communication.
17. E. V. Benton, R. P. Henke, R. G. Richmond, *Radiat. Eff.* **3**, 39 (1970); the more recent data is from E. V. Benton and R. P. Henke (paper

presented at the 7th International Colloquium on Corpuscular Photography and Visual Solid Detectors, Barcelona, July 1970).
18. W. Haymaker *et al.*, *Aerosp. Med.* **41**, 989 (1970).
19. R. W. Young, *Sci. Amer.* **223**, 81 (October 1970); W. Haymaker, paper presented at the Ames Conference, Moffett Field, Calif., June 1970.
20. We thank C. P. Bean and J. A. Bergeron of General Electric, V. Bond of Brookhaven National Laboratory, and W. Haymaker of Ames Research Center for helpful discussions; M. Fulkerson and T. Pappus of Raven Industries for balloon flights of Apollo control helmets; K. C. Hsieh of the University of Chicago for communicating the recent Climax neutron monitor results; and R. L. Golden of the NASA Manned Spacecraft Center for cheerfully dealing with an astonishing variety of official obfuscation. Supported in part by NASA under contract NAS 9-9828.
* Present address: University of California, Berkeley 94720.
27 November 1970

Geomagnetic Reversals during the Phanerozoic

Abstract. *An analysis of worldwide paleomagnetic measurements suggests a periodicity of 350 × 10⁶ years in the polarity of the geomagnetic field. During the Mesozoic it is predominantly normal, whereas during the Upper Paleozoic it is predominantly reversed. Although geomagnetic reversals occur at different rates throughout the Phanerozoic, there appears to be no clear correlation between biological evolutionary rates and reversal frequency.*

That the earth's magnetic field has reversed itself frequently in the past is now well documented (*1*). A geomagnetic polarity time scale has been established for the past 4.5 × 10^6 years by measuring the ages and magnetic polarities of volcanic rocks from many parts of the world (*2*). This time scale indicates that polarity changes occurred at a rate of about 5 per 10^6 years during the Late Tertiary. The application of the sea-floor spreading hypothesis (*3*) to marine magnetic anomalies on the basis of the Vine-Matthews crustal model (*4*) has led to the establishment of a geomagnetic polarity time scale for the whole of the Cenozoic (*5*). This time scale indicates that frequent reversals occurred during the Tertiary at a rate of about 3 per 10^6 years back to about 40 × 10^6 years ago, reducing to 1 per 10^6 years during the Early Tertiary. On the other hand, the Late Carboniferous and most of the Permian cover a period of about 50 × 10^6 years, a period during which virtually no reversals occurred and which has been termed the Kiaman magnetic interval (*6*). The reality of this long reversed epoch has been confirmed by extensive measurements in the United States and Russia (*7*). The Cretaceous has also been identified as a period during which reversals occurred only very occasionally (*8*). In this report I present an analysis of all the paleomagnetic polarity measurements for the Phanerozoic in an attempt to establish some overall pattern in the behavior of the geomagnetic field.

Data for each geological period have been compiled from the tables of paleomagnetic results of Irving (*9*), which include all results up to 1963, and from subsequent lists produced by McElhinny (*10*) which include all results from 1964 to 1969. Added to these are 22 polarity results from the Cretaceous of the United States listed by Helsley and Steiner (*8*). In addition, results have been included from the synoptic tables of the Russian paleomagnetic data (*11*), although it is difficult to decide in some cases which of these results have also been included in the other tables. There is the possibility that a small amount of duplication has occurred, but this will be unlikely to affect the conclusions drawn. In the analysis each entry in the tables of results was assigned unit weight, except that those entries which are a combination of others were excluded, as were those for which the magnetization either is known to have been acquired at a later date or is thought by the authors not to relate to the time of formation of the rock. This analysis of 1094 paleomagnetic results for the Phanerozoic is summarized by geological periods in Table 1. Where the precise ages of some igneous rocks are best known from isotopic dates, I have assigned these ages to the various geological periods, using the time scale of the Geological Society of London (*12*).

Each paleomagnetic result may be classified either as having normal polarity (N) where the magnetization is in the same sense as the present geomagnetic field, or as having reversed polarity (R) when the magnetization is in the opposite sense. In many instances both polarities occur in the one rock unit under investigation, in which case the result is listed as mixed (M). It is unlikely that paleomagnetic investigations will represent observations of the polarity over equal lengths of time. The investigations will represent the polarity over a range of intervals, and it might reasonably be assumed that this range of intervals will be approximately similar from one geologic period to the next. The observation of mixed polarities then gives some indication of the frequency with which reversals took

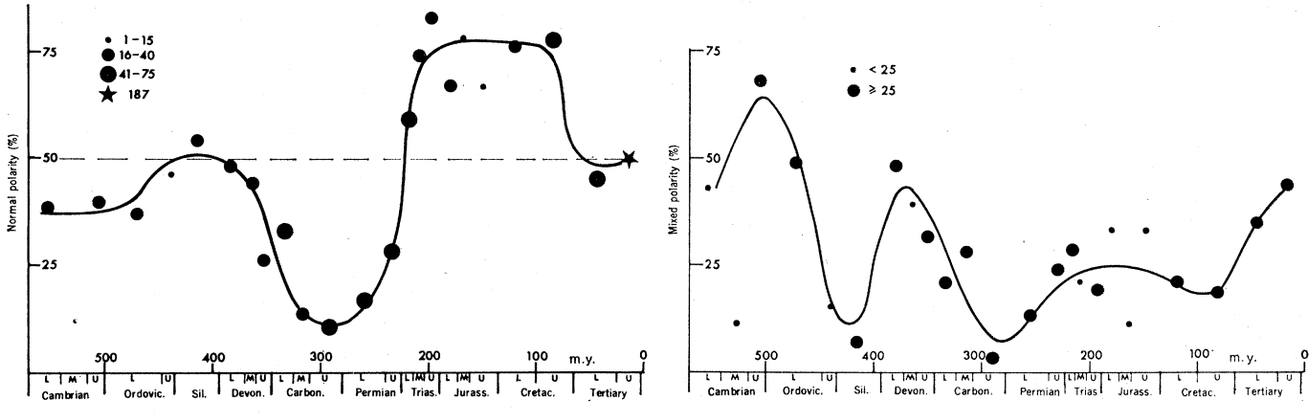

Fig. 1 (left). Percentage of normal polarity observed in worldwide paleomagnetic investigations for the Phanerozoic. The different symbols refer to the number of observations. Fig. 2 (right). Percentage of mixed polarity observed in worldwide paleomagnetic investigations for the Phanerozoic. The different symbols refer to the total number of observations.